Desalination and Water Treatment
www.deswater.com
doi: 10.5004/dwt.2021.27192

224 (2021) 433–448
June

Exploring the usability of *Cedrus deodara* sawdust for decontamination of wastewater containing crystal violet dye

Maryam Batool[a,*], Tariq Javed[a,*], Muhammad Wasim[b], Shagufta Zafar[c], Muhammad Imran Din[d]

[a]*Department of Chemistry, University of Sahiwal, Sahiwal 57000, Pakistan, emails: maryambatool6666@gmail.com (M. Batool), mtariq@uosahiwal.edu.pk (T. Javed)*
[b]*Department of Chemistry, Government Post Graduate College Jhelum, Pakistan, email: Muhammadwasim556@gmail.com*
[c]*Department of Chemistry, The Government Sadiq College Women University, Bahawalpur 63000, Pakistan, email: shg_zf@yahoo.com*
[d]*Institute of Chemistry, University of the Punjab Lahore, Pakistan, email: imran.chem@pu.edu.pk*

Received 24 August 2020; Accepted 27 February 2021

ABSTRACT

This study centers on crystal violet removal from raw water on surface of *Cedrus deodara* sawdust. Main objectives of this study are to investigate the potential of *Cedrus deodara* sawdust for removal of toxic crystal violet dye and to stimulate the best experimental conditions. Adsorption parameters, isotherms, kinetic equations, and thermodynamics have been studied and discussed. Experiments were performed to investigate the effects of various parameters, that is, size of adsorbent, pH, adsorbent dose, contact time, dye concentration and temperature on dye exclusion. Isotherms, that is, Langmuir, Freundlich and Dubinin–Radushkevich isotherms and kinetic models, that is, pseudo-first-order, pseudo-second-order and intraparticle diffusion models have been applied and discussed. Thermodynamic parameters, that is, change in Gibbs free energy, enthalpy and entropy have also been determined. Maximum amount of dye (99.21%) has been removed at optimized conditions, that is, 210 mesh size, 50°C temperature, pH 12, 0.4 g adsorbent, 20 ppm adsorbate concentration with contact time of 30 min. Data fits best to Langmuir isotherm and process obeys pseudo-second-order kinetics. Calculated free energy and enthalpy indicates spontaneity and endothermicity of the process. Applicability of developed procedure with tap water is 92% indicating that *Cedrus deodara* is an auspicious adsorbent for crystal violet removal from water.

Keywords: Cedrus deodara sawdust; Crystal violet; Adsorption; Isotherms; Kinetics; Desorption

1. Introduction

Dyes are organic compounds, may be natural or artificial, that become attached to the surface of fabric giving it bright color and are used in many industries [1] but they have toxic and carcinogenic nature [2–4]. There are more than 10,000 commercially available dyes and approximately 7×10^5 tonnes of colorants are produced yearly all over the world [2,5–8]. Almost 2% of dyes are liberated into water-bodies leading to water pollution [2,9]. Toxicity of cationic dyes is more than anionic ones. This is due to the fact that cationic dyes interact more rapidly with negatively charged surface of cell membrane than anionic ones leading to suffocation and skin allergies [10,11].

Crystal violet dye also known as basic violet 3 (for structural formula of crystal violet dye see Fig. 1) is one of the most widely used cationic dye [12]. In water, it appears violet blue and it is λ_{max} was found to be 590 nm

* Corresponding author.

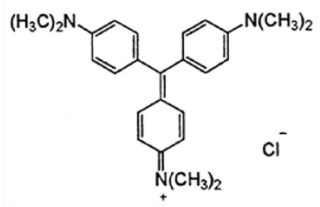

Fig. 1. The structural formula of crystal violet dye.

with extinction coefficient of 87,000 M^{-1} cm^{-1}. Hue of dye depends on pH of solution. It appears green at pH 1, having λ_{max} = 20 and 620 nm. In highly acidic solutions, it is yellow with λ_{max} = 420 nm [9].

It is widely used in paint, printing ink and veterinary medicines etc. It also manifests antibacterial and antifungal characteristics [13]. It is useful for the treatment of burns, boils, carbuncles, mycotic skin infections [14] and in many industrial processes such as dyeing various textiles (e.g., cotton, silk, nylon and wool), oils and waxes, paper and plastics etc. [15,16]. However, when these dyes are ejected into water stream directly (devoid of any proper handling), they result in deterioration of water quality as they remained in environment for a long time [17]. Crystal violet causes breathing difficulties, eye burns, nausea, oral ulceration [18,19] cancer [17], jaundice, tissue necrosis, shock, kidney failure [20], permanent injury to cornea and conjunctiva [15] and digestive tract irritation [13,17,21].

For preserving water resources [22–26] and protecting human health, various methods such as ozonation, electro-coagulation, membrane process, biological, and solvent extraction methods are used for water treatment. However, adsorption method is widely used and the most effective process for dyes removal because of its simple design, effectiveness, easy operation, economic feasibility, insensitivity towards toxic substances and easy availability of adsorbents used for adsorption at low cost [9].

How do we meet the needs to current and future generations? Such as healthcare problems, preservation, and protection of natural resources (such as water, air, and soil), for environment protection and sustainability. This article focuses on the purpose to investigate the role of *Cedrus deodara* sawdust for degradation, decolorization and removal of toxic crystal violet dye from textile effluents. Research objectives include, investigating the use of *Cedrus deodara* sawdust for decolorization of crystal violet dye from wastewater, to optimize adsorption parameters for efficient dye removal and to determine dye decolorization kinetics, isotherm models and thermodynamic parameters. Novelty of this article is that till yet no work has been reported on crystal violet dye removal using *Cedrus deodara* sawdust (specifically) as an adsorbent.

2. Methods and experimentation

2.1. Apparatus and chemicals

Chemicals used throughout the experiment are of systematic value. Distilled water was used throughout the research work. Apparatus/instruments required during whole process include UV-Vis spectrophotometer, scanning electron microscope (SEM), Fourier-transform infrared (FTIR) spectrophotometer, centrifugation machine, microwave oven, pH meter, weighing balance and hot plate.

2.2. Preparation of adsorbate solution

Analytical grade crystal violet dye with molecular formula $C_{25}H_{30}ClN_3$ and molecular mass 407.979 g mol^{-1} was obtained from laboratory and 1,000 ppm dye stock solution was prepared by dissolving 1 g of it in 1 L of purified water (Fig. 2) which was then further diluted according to requirement.

2.3. Collection of adsorbents

Cedrus deodara sawdust (CDS) was collected from a furniture shop which was then dried and ground into small fine pieces (Fig. 3) to increase its surface area. Sieving was done to obtain particles of various mesh sizes, that is, 105, 210 and 500 mesh sizes which were then finally stockpiled in airtight plastic boxes to use in further experiments.

2.4. Batch adsorption studies

For optimization of various adsorption parameters, such as pH (1, 2, 3, 4, 5, 6, 7, 8, 9, 10, 11 and 12), adsorbent dose (0.1, 0.2, 0.4, 0.5, 0.6, 0.8 and 1.00 g), adsorbate concentration (5, 10, 20, 30, 40, 50, 60, 80 and 100 ppm), exposure time (5, 10, 20, 30, 40, 50, 60, 80, 100 and 120 min) and temperature (0°C, 10°C, 20°C, 30°C, 40°C and 50°C), batch adsorption experiment was carried out.

Experiments were performed by manipulating only one adsorption parameter at a time while keeping others constant. Initial concentration of dye was determined before adsorption by UV-Vis spectrophotometer at a wavelength of 574 nm. Centrifugation after manual shaking was completed and amount of dye present in supernatant was determined by absorbance measurement again at 574 nm using UV-Vis spectrophotometer. Formula used for dye uptake is given in Eq. (1):

$$\%\text{age removal} = \frac{A_i - A_f}{A_i} \times 100 \tag{1}$$

where A_i = initial absorbance before dye adsorption and A_f = final absorbance after dye adsorption. Adsorption capacity q_t (mg g^{-1}) was determined by formula given in Eq. (2):

$$q_t = \frac{\left(C_0 - C_e\right)V}{M} \tag{2}$$

where C_0 (mg L^{-1}), C_e (mg L^{-1}) are initial and equilibrium concentrations of dye respectively, V is volume of dye solution taken and M is the molar mass of adsorbent.

3. Adsorbent characterization

FTIR and SEM techniques were used for adsorbent characterization on the way to determine functional groups

Fig. 2. Crystal violet dye in solution form.

Fig. 3. The powder form of *Cedrus deodara* sawdust.

(present at the surface of adsorbent) and to study texture and morphology of adsorbent, respectively. FTIR study of adsorbent was made by making 1% pallet of potassium bromide (KBr). Scale for this study was in the spectral range of 4,000–400 cm^{-1} [27]. For SEM analysis, sample was prepared by grinding adsorbent in pestle and mortar followed by sieving. Sample was then affixed on double sided carbon tape present on taster holders [28]. Scanning electron microscope analysis of adsorbent before and after adsorption was carried out by using (JEOL, JSM-6510LV, Japan) [27].

Complete research methodology involves following steps: Firstly, preparation, that is, collection, grinding, sieving, storage of adsorbent and preparation of crystal violet dye stock solution. Secondly, adsorption step in which adsorption of crystal violet dye onto the surface of *Cedrus deodara* sawdust under different conditions of solution pH, adsorbent dosage, contact time, adsorbate concentration and temperature were studied. Lastly, analysis step involved the determination of removal efficiency of *Cedrus deodara* sawdust towards crystal violet dye and measurement of initial and final absorbance by UV-Vis Spectrophotometer.

4. Results and discussion

4.1. Description of adsorbent

Results of FTIR analysis of dye unloaded and dye loaded adsorbents are given in Fig. 4:

FTIR analysis confirmed that the functional groups such as carboxyl, hydroxyl and carbonyl etc. contribute mainly to crystal violet dye adsorption onto the surface of *Cedrus deodara* sawdust. Strong bands ranges from 3,600–3,200 cm^{-1}, 3,000–2,850 cm^{-1}, broadband peak at 3,396 cm^{-1} and peak at 2,912 cm^{-1} correspond to stretching vibrations of hydroxyl group and adsorbed water, C–H stretching vibrations of alkane group, O–H stretching of alcoholic group, C–H stretching of an alkane correspondingly. Band in 1,730 and 1,635 cm^{-1} agree to C=O non-ionic and ionic stretching of carboxyl groups, respectively. Peak at 1,037 cm^{-1} correspond to C–N stretching of amine group and OH stretching of carbohydrate. After dye uptake, there was a shift in peaks from 3,396–3,421 cm^{-1}, 2,912–2,920 cm^{-1}, 1,635–1,614 cm^{-1}, 1,037–1,023 cm^{-1}. All peaks of the functional groups involved in dye uptake became diminished after dye uptake. This confirmed the active participation of alcoholic and carboxylic groups in crystal violet dye adsorption [27].

SEM photographs of dye unloaded, and dye loaded adsorbent are given in Figs. 5 and 6 respectively:

SEM analysis showed that the surface of adsorbent is highly rough, diverse, and porous indicating increased superficial zone of adsorbent accessible for adsorption of crystal violet dye. After adsorption, these pores were occupied by dye molecules resulting in dye exclusion [27].

4.2. Effects of pH

Adsorption behavior of crystal violet dye on surface of *Cedrus deodara* sawdust was investigated at different pH's of solution. From experimental work (Table S1), it became clear that dye adsorption is directly related with solution pH, that is, at solution pH of 12; percentage removal of dye was 88.88%. There as on behind this is that at high pH, exterior of adsorbent material was negative (due to deprotonation of functional groups present on the surface of adsorbent) on which positive ions of dye molecules adsorb hastily due to electrostatic interactions between oppositely charged ions. While a low pH leads to desorption of dye molecules due to repulsions between positively charged ions of dye molecules and the surface of adsorbent. Graph to study the effect of solution pH on adsorption is shown in (Fig. 7).

An adsorbent characteristic known as point of zero charge (pH_{pzc}) better explain the effects of pH on adsorption phenomenon. pH_{pzc} of adsorbent was found to be 8 which showed that the surface of adsorbent was positive when pH < 8 (due to protonation of functional groups) and when pH ≥ 8, the surface of adsorbent becomes negatively charged due to deprotonation of functional groups on the surface of adsorbent due to the presence of excess of hydroxyl ions at high pH. Thus pH_{pzc} of 8 showed that *Cedrus deodara*

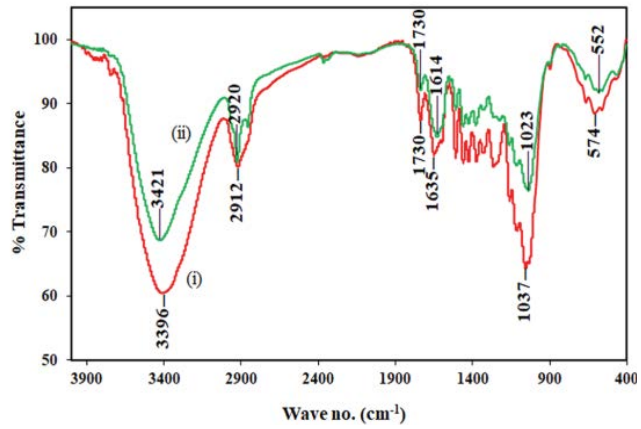

Fig. 4. FTIR spectra of dye unloaded (i) and loaded (ii) *Cedrus deodara* sawdust. It confirms the involvement of OH^- and COO^- groups of adsorbents in dye adsorption.

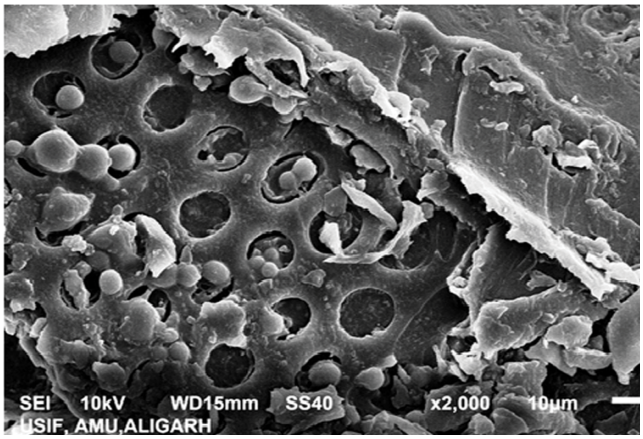

Fig. 6. SEM micrograph (with a magnification of 2,000 times of dye loaded *Cedrus deodara* sawdust in which all pores of surface are occupied by dye molecules.

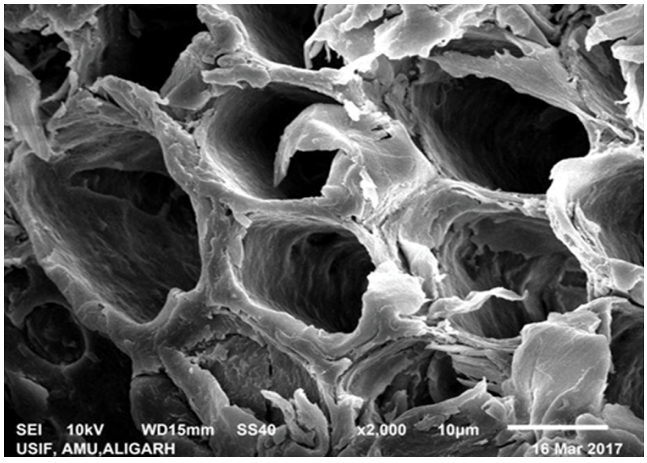

Fig. 5. SEM micrograph (with a magnification of 2,000 times) of dye unloaded *Cedrus deodara* sawdust showing the porous surface of the adsorbent.

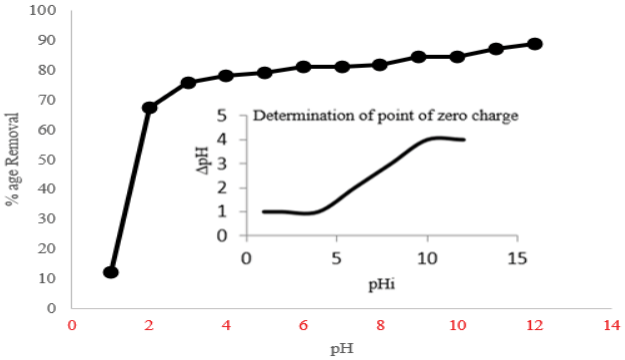

Fig. 7. Plot of pH against % age removal (experimental conditions: pH = variable (1–12); C_0 = 10 ppm; adsorbent dose = 0.25 g; contact time = 20 min; temperature = 25°C). Inner small graph shows the determination of point of zero charge.

sawdust could adsorb any cationic dye efficiently at pH equal to or above 8 [27].

4.3. Effects of adsorbent dose

To investigate the consequences of adsorbent dose in exclusion efficacy of crystal violet dye, adsorbent dose varied from 0.1 to 1.00 g. With rise in adsorbent amount, percentage removal of crystal violet dye increases constantly up to 0.4 g (with 98.03% dye removal) after which it became constant (graph is shown in Fig. 8). The upswing in removal percentage with increase in adsorbent dose owned to increase in number of available adsorption spots at exterior of adsorbent. Results of experiment to study the effects of adsorbent dosage are given (Table S2).

4.4. Effects of contact time

Contact time is the time taken by an adsorbate for complete adsorption of dye onto the surface of adsorbent. To examine the effects of contact time on adsorption process of crystal violet dye, different series of exposure time were carefully chosen, that is, from 5 to 120 min. From experiments, it became clear that equilibrium time for adsorption of crystal violet dye on exterior of *Cedrus deodara* sawdust was 120 min resulting in 96.24% of dye removal. However, at the contact time of 30 min, % age removal was 93.65%. Since there is not much difference in removal efficiency after 30 and 120 min so, we selected 30 min for the next experiments to conserve both energy and time (graph of experiment is shown in Fig. 9). Fast reaction in beginning was due to the presence of vacant adsorption spots at exterior of adsorbent. After some time, all vacant sites were occupied resulting in small increase in dye removal. Results of experiment to study the effects of contact time are given in Table S3.

4.5. Effects of adsorbate concentration

Consequences of adsorbate concentration on adsorption were studied by altering adsorbate dosage from 5 to 100 ppm. At pH 12, 0.4 g of *Cedrus deodara* sawdust was taken and varied amount of adsorbate (with exposure

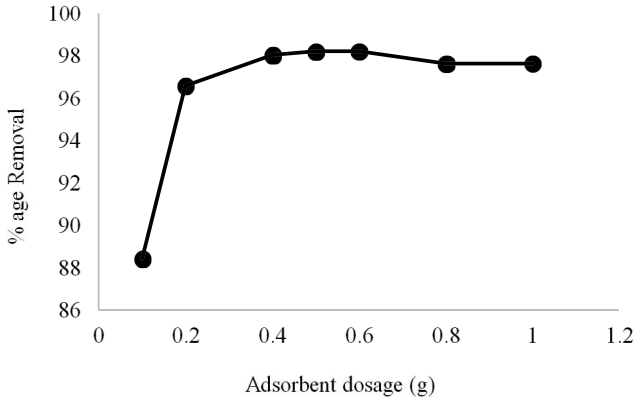

Fig. 8. Plot of adsorbent dose against % age removal (experimental conditions: adsorbent dose = variable (0.1–1.0 g); pH = 12; C_0 = 40 ppm; contact time = 20 min; temperature = 25°C).

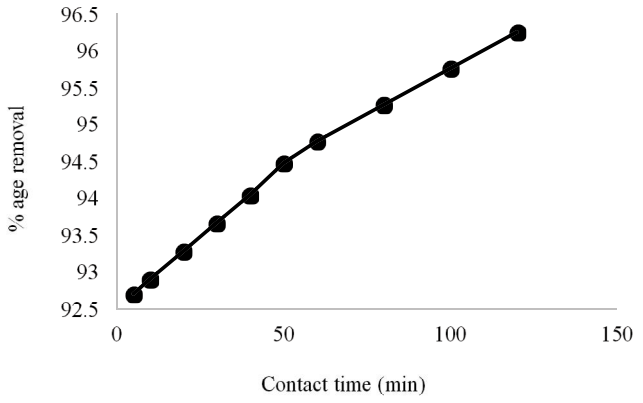

Fig. 9. Plot of contact time against % age removal (experimental conditions: contact time = variable (05–120 min); pH = 12; adsorbent dose = 0.4 g; C_0 = 80 ppm; temperature = 25°C).

time of 30 min) was used to study the removal efficiency of adsorbent towards crystal violet dye. From experiments, it became clear that % age removal remain almost constant, that is, 99% from 5 to 20 ppm. From 20 to 100 ppm removal percentage decreases constantly from 99% to 98% (graph is shown in Fig. 10). Initial increase in removal efficiency was due to the excess quantity of adsorbate which get adsorbed onto the surface of adsorbent quickly resulting in maximum removal of dye. When all active spots are fully filled by dye particles then there was no such further increase in dye removal. Results of experiment to study the effects of dye concentration are given in Table S4.

4.6. Effects of temperature

Temperature influence on adsorption process of crystal violet at optimized conditions has also been studied. From temperature effect thermodynamic parameters can be determined, that is, we can determine whether the process was spontaneous or non-spontaneous, endothermic, or exothermic and whether it cause rise or fall in entropy. From experiments, it became clear that percentage

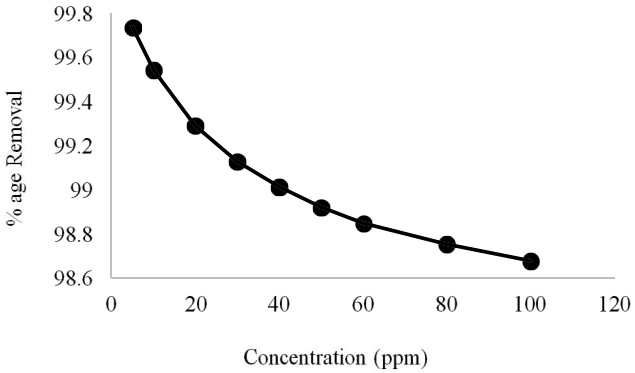

Fig. 10. Plot of dye conc. against % age removal (experimental conditions: C_0 = variable (05–100 ppm); pH = 12; adsorbent dose = 0.4 g; contact time = 30 min; temperature = 25°C).

removal increases continuously from 98% to 99% when the temperature was expanded from 0°C to 50°C (graph is shown in Fig. 11). At low temperature, dye molecules preferred to remain in solution rather than onto the surface of adsorbent. At high temperature, dye molecules moved from solution to the surface of adsorbent resulting in maximal dye removal indicating that the procedure was endothermic, that is, dye removal is directly proportional to temperature. Main reason behind this was that at high temperature, kinetic energy of the molecules increases consequently, dye particles move from solution towards the adsorbent surface causing maximum adsorption of dye on the surface of adsorbent. Results of experiment to study the effects of temperature are given in Table S5.

4.7. Adsorption kinetics

Study of reaction kinetics is important for the determination of optimum exposure time for adsorption and its mechanism. Various kinetic models have been employed on investigational records to examine the mechanism of adsorption and these include, pseudo-first-order, pseudo-second-order and intraparticle diffusion model. Pseudo-first-order and pseudo-second-order kinetic models are useful for rate determining steps while intraparticle diffusion model is useful to study the kinetic mechanism of adsorption [28].

4.7.1. Kinetic models

4.7.1.1. Pseudo-first-order kinetic model (Lagergren model)

This model states that: rate of sorption is directly related to the number of free adsorption spots [28] and it is expressed in Eq. (3):

$$\frac{dq_t}{dt} = k_f\left(q_e - q_t\right) \tag{3}$$

where q_t (mg g^{-1}) is amount of adsorbate adsorbed at time 't', q_e (mg g^{-1}) is amount of adsorbate adsorbed at equipoise time and k_f is pseudo-first-order rate constant. Linear form of pseudo-first-order by Lagergren is given in Eq. (4):

$$\ln\left(q_e - q_t\right) = \ln q_e - k_f t \tag{4}$$

A straight line graph is obtained when $\ln(q_e - q_t)$ is plotted against t (min) and slope k_f and intercept q_e can be determined from this graph [29]. From experiments (graph is shown in Fig. 12) it became clear that current adsorption process does not go along with pseudo-first-order kinetics. Since, experimentally determined value of q_e was 1.90494 mg g^{-1} and calculated value was 0.025 mg g^{-1}. Furthermore, value of R^2 = 0.48 which is very less than unity indicating poor rate of reaction. Investigational statistics for pseudo-first-order kinetics is given in Table S6.

4.7.1.2. Pseudo-second-order kinetic model

According to this model, chemical sorption is a rate controlling step. Pseudo-second-order mathematical expression is given in Eq. (5):

$$\frac{dq_t}{dt} = k_s\left(q_e - q_t\right)^2 \tag{5}$$

where q_t (mg g^{-1}) is amount of adsorbate adsorbed at time 't', q_e (mg g^{-1}) is amount of adsorbate adsorbed at equilibrium and k_s (g mg^{-1} min^{-1}) is pseudo-second-order rate constant. Linear form of this equation is given in Eq. (6):

$$\frac{t}{q_t} = \frac{1}{k_s q_e^2} + \frac{t}{q_e} \tag{6}$$

A plot of t/q_t (min g mg^{-1}) in contrast to t (min) yield a straight line from which slope and intercept can be calculated [29]. For second-order kinetics (graph is shown in Fig. 13), experimentally determined value of q_e was 1.904 mg g^{-1} and calculated q_e was 1.908 mg g^{-1} which is very close to investigational quantity. Also, value of R^2 was 0.9999 (very close to 1) which means that the process follows pseudo-second-order kinetics. Investigational statistics for pseudo-second-order kinetics is shown in Table S7.

4.7.1.3. Intraparticle diffusion model

This model was established by Weber and Morris for determining the diffusion mechanism and rate controlling step and can be expressed in Eq. (7):

$$q_t = K_{\text{id}} t_{0.5} + I \tag{7}$$

where q_t (mg g^{-1}) is amount of adsorbate adsorbed at time 't', I is the thickness of layer and K_{id} (mg g^{-1} $min^{-1/2}$) is intraparticle diffusion constant. A straight line is obtained when a graph is plotted between q_t and $t_{0.5}$ and slope K_{id} and intercept 'I' can be obtained from this graph [29]. In case of intraparticle diffusion model, a linear graph shows that only intraparticle diffusion model is involved in adsorption procedure and zero intercept shows that this model is rate limiting step. When the line doesn't pass by way of origin (graph is shown in Fig. 14), it confirms some extent of boundary layer management and also that intraparticle diffusion model is not only rate controlling step but other kinetic models are also engaged in the management of adsorption level [28]. Investigational statistics for intraparticle diffusion model is given in Table S8.

Comparison of different kinetic models is given in Table 1. From table it is concluded that process follows

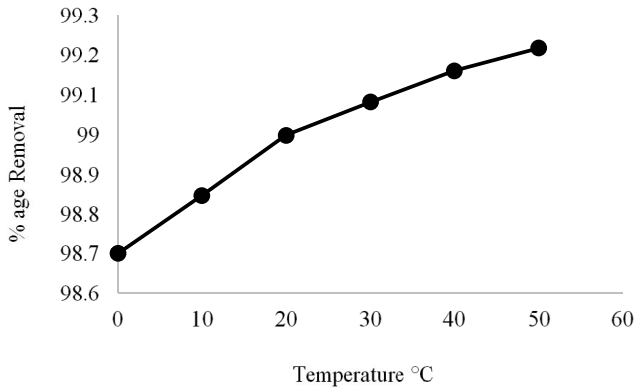

Fig. 11. Plot of temperature against % age removal (experimental conditions: temperature = variable (0°C–50°C); pH = 12; adsorbent dose = 0.4 g; contact time = 30 min; C_0 = 200 ppm).

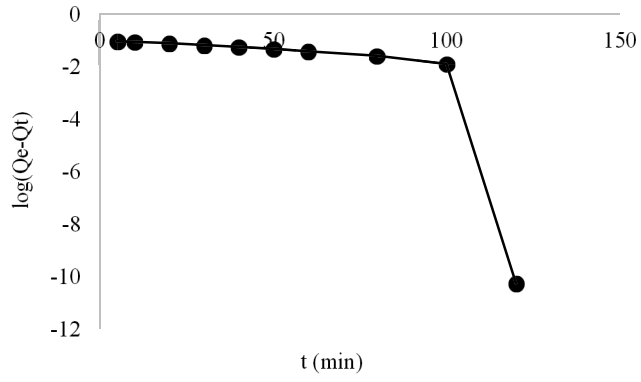

Fig. 12. Graph for the pseudo-first-order kinetic model.

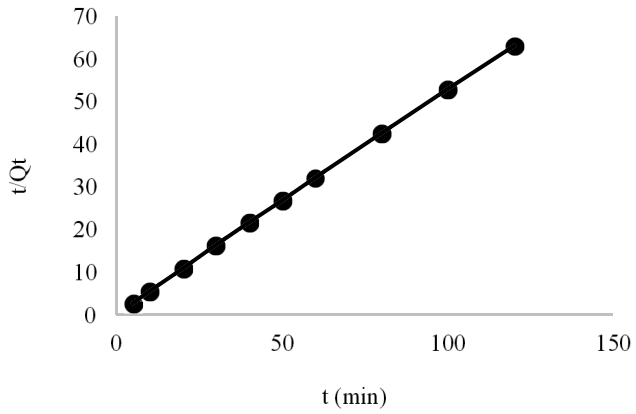

Fig. 13. Graph for the pseudo-second-order kinetic model.

pseudo-second-order kinetic model rather than pseudo-first and intraparticle diffusion model since value of regression coefficient for pseudo-first-order is 0.48 while it is 0.9999 for pseudo-second-order kinetic model (which is very close to unity). Further more experimental q_e (mg g^{-1}) and calculated q_e (mg g^{-1}) in case of pseudo-second-order model are in good agreement than pseudo-first and intraparticle diffusion model. This comparison confirms that process follows pseudo-second-order kinetic model.

4.8. Adsorption isotherm models

Complete quantification of adsorption process is required during its applicability on commercial level. These mathematical models [28] describe adsorbent–adsorbate interactions and the adsorption capacity [30]. For this purpose, concentration data from experiments is analyzed using various isotherm models to determine the best suited isotherm model in the adsorption process. Isotherm models applied here include, Langmuir, Freundlich and Dubinin–Radushkevich isotherm.

4.8.1. Isotherm models

The results of different isotherm models are given below:

4.8.1.1. Langmuir adsorption isotherm model

Irving Langmuir received a noble prize in 1916 due to his work on surface chemistry. Basic assumptions of this isotherm model include [28,29].

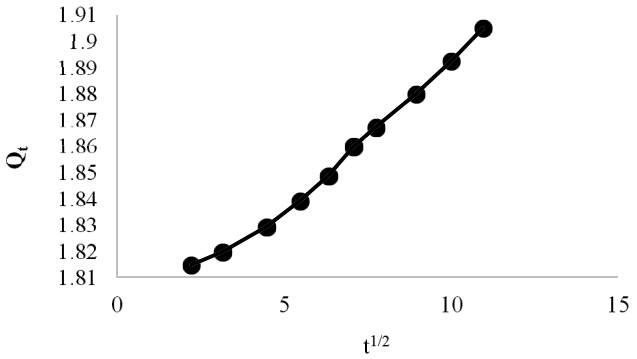

Fig. 14. The plot between $t^{1/2}$ and Q_t for intraparticle diffusion kinetic model.

- Adsorbent exterior has definite number of adsorption sites.
- No interactions exist between the molecules adsorbed on exterior of an adsorbent.
- It involves the development of a monolayer of molecules on surface of the material.

For monolayer adsorption, chemical reaction might be written as given in Eq. (8):

$$A_{(g)} + S \rightarrow AS \tag{8}$$

where '*A*' is gas molecule and '*S*' is an adsorbed location on the surface of an adsorbent. For this reaction, equilibrium constant is given in Eq. (9):

$$K_{\text{ads}} = \frac{[AS]}{[A][S]} \tag{9}$$

Langmuir isotherm can be completely defined in relationships of surface coverage θ (Eqs. (10) and (11)) which is well-defined as fraction of the adsorption spots unavailable at equipoise.

$$K = \frac{K}{K_{-1}} = \frac{\theta}{(1-\theta)P} \tag{10}$$

$$\theta = \frac{KP}{1+KP} \tag{11}$$

where K and K_{-1} are direct and converse rate constants and '*p*' is partial pressure of gas. Amount of gas adsorbed on the substance is usually given in moles gram. For solution, above equation takes the form given in Eq. (12):

$$q_e = \frac{K_L C_e q_m}{1 + K_L + C_e} \tag{12}$$

Linear form of this equation is given in Eq. (13):

$$\frac{1}{q_e} = \frac{1}{q_{\max}} + \left(\frac{1}{q_{\max} K_L}\right)\frac{1}{C_e} \tag{13}$$

where K_L is Langmuir constant (dm^{-3} mol^{-1}) and $q_{\max}$ is monolayer Langmuir adsorption capacity (mg g^{-1}). Simplest form of above equation is given in Eq. (14):

Table 1
Comparison of kinetic parameters of three models (pseudo-first-order, pseudo-second-order, and intraparticle diffusion model)

Pseudo-first-order	Pseudo-second-order	Intraparticle diffusion model
Adsorbate conc. (mg L^{-1}): 20	Adsorbate conc. (mg L^{-1}): 20	Adsorbate conc. (mg L^{-1}): 20
Experimental q_e (mg g^{-1}): 1.904	Experimental q_e (mg g^{-1}): 1.904	Experimental q_e (mg g^{-1}): 1.904
Computed q_e (mg g^{-1}): 0.025	Computed q_e (mg g^{-1}): 1.908	Computed q_e (mg g^{-1}): 1.785
R^2: 0.48	R^2: 0.999	R^2: 0.989
k_1 (min^{-1}): 0.117	k_1 (min^{-1}): 0.5911	K_{id}: 0.0106

$$\frac{C_e}{q_e} = \frac{1}{q_{\max} K_L} + \frac{C_e}{q_{\max}} \tag{14}$$

When a graph is plotted between C_e (mg L^{-1})/q_e (mg g^{-1}) and C_e (mg L^{-1}) then a straight line is obtained from which slope and intercept can be calculated [29]. From experiments (graph is shown in Fig. 15) it was found that value of R^2 for Langmuir isotherm was 0.9994 (very close to unity) indicating that current process of adsorption is favorable. It showed that first layer of molecules adsorbed on the surface of adsorbent with energy almost equal to the energy of heat of adsorption for monolayer adsorption [17]. A dimensionless constant 'separation factor' parameter, 'R_L' determines whether the adsorption process is favorable ($0 < R_L < 1$), unfavorable ($R_L > 1$), linear ($R_L = 1$) or irreversible ($R_L = 0$). It is given in Eq. (15):

$$R_L = \frac{1}{1 + bC_{\text{In}}} \tag{15}$$

where b = (L mol^{-1}) is Langmuir adsorption equilibrium constant and C_{In} = (mol L^{-1}) is initial dye concentration. Values of R_L were calculated by Langmuir constant 'b' and adsorbate concentration. From values of R_L (Table S9), it became clear that the adsorption procedure of crystal violet onto the surface of *Cedrus deodara* sawdust was linear process since all the values of R_L are unity. Experimental data for Langmuir isotherm model is given in Table S10.

4.8.1.2. Freundlich adsorption isotherm model

An experimental calculation that represents adsorption data is called Freundlich equation [28]. According to this model, quantity of adsorbate adsorbed on exterior of an adsorbent is directly proportional to the pressure of gas and is given in Eq. (16):

$$q_e = K_F P \tag{16}$$

When pressure of gas changes then above equation can be written as in Eq. (17):

$$q_e = K_F P^{1/n} \tag{17}$$

Taking antilog of above equation, we get linear formula of Freundlich isotherm given in Eq. (18):

$$\ln q_e = \ln K_F + \frac{1}{n} \ln P \tag{18}$$

In case of solutions, above equation can be written in Eq. (19):

$$\ln q_e = \ln K_F + \frac{1}{n} \ln C_e \tag{19}$$

where K_F is Freundlich constant, n is the slope and q_e (mg g^{-1}) is quantity of adsorbate adsorbed on each gram of an adsorbent. A plot of $\ln q_e$ in contrast to $\ln C_e$ results in a straight line graph and value of slope $1/n$ gives us the value of 'n' and intercept $\ln K_F$ gives the value of K_F. When value of 'n' is more than unity, it means adsorption proceeds to a greater amount. Value of 'n' varies from 1 to 10^{19} [29]. This adsorption isotherm has the advantage that it involves multilayer adsorption and there is no limitation in the amount of a substance adsorbed [28]. Value of K_F in case of Freundlich isotherm (from experimental graph shown in Fig. 16) was 5.288×10^9 and that of R^2 was 0.9694. Experimental data for Freundlich isotherm model is given in Table S11.

4.8.1.3. Dubinin–Radushkevich isotherm model

This isotherm model was developed by Dubinin–Radushkevich which is applied to calculate apparent energy of adsorption. Basic equation of this model is given in Eq. (20):

$$\ln q_e = \ln q_{\text{DR}} - \beta\varepsilon^2 \tag{20}$$

where β is an activity coefficient, q_{DR} is the imaginary inundation capacity and ε is the Polanyi potential and is given in Eq. (21):

$$\varepsilon = RT \ln\left(1 + \frac{1}{C_e}\right) \tag{21}$$

where T is the temperature and R is general gas constant [29]. From value of β, mean sorption energy is well-defined

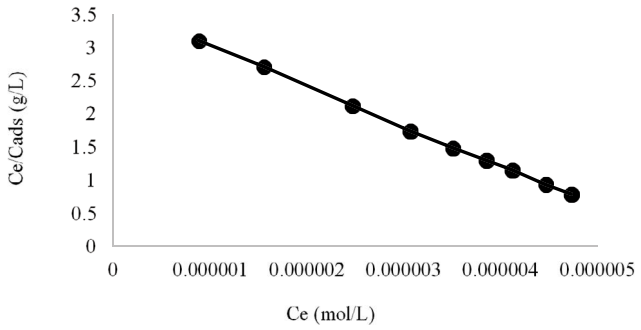

Fig. 15. Graph for Langmuir isotherm.

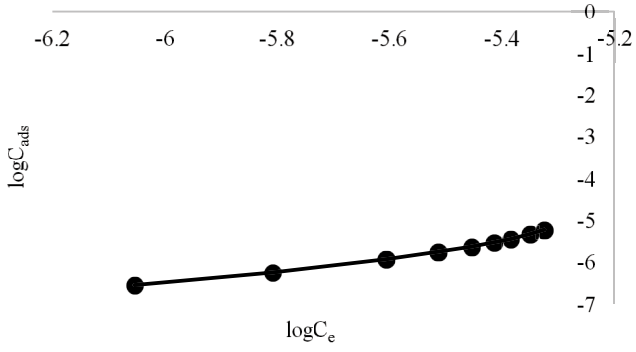

Fig. 16. Graph for Freundlich isotherm.

as energy of transfer of one mole of solute from infinity to the exterior of an adsorbent [28] and can be calculated by equation given in Eq. (22):

$$E_s = \frac{1}{\sqrt{2\beta}} \tag{22}$$

From Dubinin–Radushkevich isotherm (as shown in Fig. 17), calculated value of β is 0.393 KJ^2 mol^{-2} and R^2 is 0.9634 which showed that the chemisorption phenomenon is also involved in adsorption of crystal violet dye. Experimental data for Dubinin–Radushkevich model is shown in Table S12.

On basis of R^2 values of different isotherm models (given in Table 2), it can be concluded that Langmuir isotherm is more appropriate than Freundlich and fits best to experimental data for crystal violet dye adsorption on *Cedrus deodara* sawdust. Value of R^2 for Langmuir isotherm is 0.9994 (very close to unity) and for Freundlich value of regression coefficient is 0.9694 which is small as compared to Langmuir isotherm model.

Comparison of adsorption capacities of different adsorbents for crystal violet dye removal is given in Table 3. Table clearly shows the variations in q_{max} (mg g^{-1}) by different adsorbents at different experimental conditions like pH and it became clear that *Cedrus deodara* sawdust is one of the most effective adsorbents for crystal violet dye removal since its q_{max} is 0.673 mg g^{-1} higher than many of adsorbents mentioned in table.

4.9. Thermodynamic parameters

Feasibility and type of adsorption could be determined from thermodynamic parameters such as Gibbs free energy change (Δ*G*), enthalpy change (Δ*H*) and entropy change (Δ*S*) of a system. From distribution coefficient, thermodynamic parameters can be calculated as given in Eq. (23):

$$K_c = \frac{C_{ad,s}}{C_{Eq,L}} \tag{23}$$

where C_{ads} is quantity of adsorbate adsorbed on solid at equipoise (mg L^{-1}) and $C_{Eq,L}$ is quantity of adsorbate left over in the solution at equipoise (mg L^{-1}). In Van't Hoff equation, K_c is related with Δ*H* and Δ*S* as given in Eq. (24):

$$\ln K_c = -\frac{\Delta H}{RT} + \frac{\Delta S}{R} \tag{24}$$

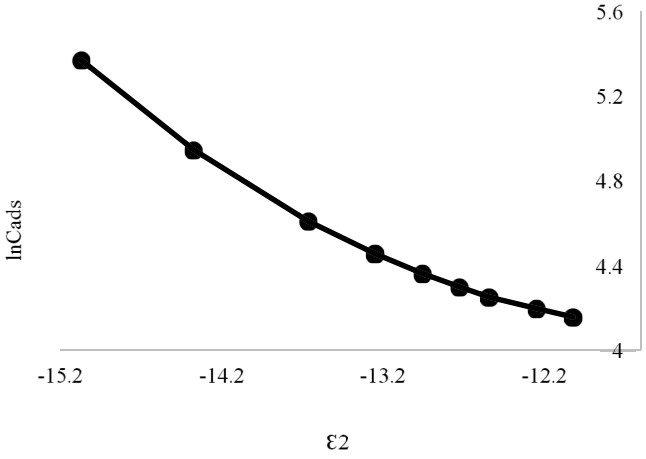

Fig. 17. Graph for Dubinin–Radushkevich isotherm.

Table 2
Parameters of isotherm models (Langmuir, Freundlich and Dubinin–Radushkevich model)

Langmuir isotherm model	Temp. (°C): 25	Q_0 (mg g^{-1}): 0.673	b (dm^3 mol^{-1}): 1.66 × 10^{-5}	R^2: 0.9994
Freundlich isotherm model	Temp. (°C): 25	k_f (mg g^{-1}): 5.288 × 10^9	n (L g^{-1}): 0.563	R^2: 0.9694
Dubinin–Radushkevich isotherm model	Temp. (°C): 25	β (KJ^2 mol^{-2}): 0.393	ε^2 (KJ mol^{-1}): –1.12	R^2: 0.9634

Table 3
Comparison of adsorption capacities of different adsorbents for crystal violet dye removal

Adsorbent	q_{max} (mg g^{-1})	pH	Reference
Cedrus deodara sawdust	0.673	12	Present study
Groundnut shell	0.524	6	[14]
Artocarpus odoratissimus (tarap) core	217	9.4	[31]
Diplazium esculentum	351	8	[32]
MWCNTs/$Mn_{0.8}Zn_{0.2}Fe_2O_4$ nanoparticles	5.00	11	[33]
Artocarpus camansi peel through sodium hydroxide treatment	479		[34]
Momordica charantia (bitter gourd) waste (BGW)	261.8		[35]
Raw cassava peels powder	–5.15	10	[9]
Date palm fibers	0.66	2	[36]
Bean pod	0.380	5	[14]
Mesocellular foam (MCF)	6.6	9	[37]

A straight-line graph is attained when we plot lnK_c in contradiction of 1/T. Slope of graph is ΔH and intercept is ΔS. Where, R is universal gas constant and is = 8.31 J mol^{-1} K^{-1} and T is temperature in Kelvin. Relation for ΔG is given in Eq. (25):

$$\Delta G = \Delta H - T\Delta S^{\circ} \text{ [28]} \quad (25)$$

From experimental results (graph is shown in Fig. 18) it became clear that the process is of endothermic nature as indicated by the positive value of ΔH. Negative values of Gibb's Free energy prove that current phenomenon is spontaneous in nature. Positive value of ΔS is an indication of increase in randomness with increase in temperature (as confirmed by calculated thermodynamic parameters given below in Table 4). Investigational statistics for thermodynamic parameters are shown in Table S13.

4.10. Applicability of developed practice with tap water

Applicability of this established practice with tap water containing various anions and cations like Cl^-, PO_4^{2-}, CO_3^{2-}, Na^+ and K^+ ions etc. using optimized conditions, that is, pH 12, 0.4 g of adsorbent dosage, providing adsorption time of 30 min with 20 ppm of initial dye concentration comes out to be 92.324%. The results of tap water treatment validate the applicability of developed procedure towards real samples.

5. Mechanism of adsorption

FTIR study explores the presence of polar functional groups such as hydroxyl, carbonyl, carboxyl etc. in *Cedrus deodara* sawdust (CDS). It also reveals that adsorption of crystal violet dye was mainly due to the presence of hydroxyl and carboxyl groups on the surface of adsorbent. Strong electrostatic forces of attraction develop between these functional groups and positively charged crystal violet dye molecules (CV^+Cl^-) resulting in its adsorption on the surface of adsorbent.

This adsorption phenomenon was highly pH dependent and high pH resulted in greater amount of dye removal. Percentage age removal of dye increased constantly with increase in solution pH due to development of strong interactions between positively charged dye molecules and negatively charged surface of adsorbent (due to presence of OH^- and COO^- OH^- and COO^- groups).

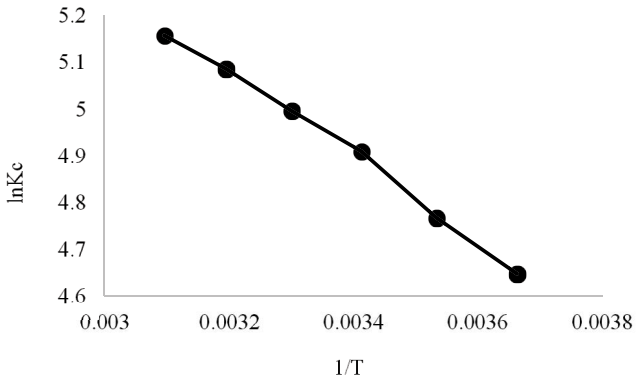

Fig. 18. Van't Hoff plot (for thermodynamic parameter calculations) indicating the process to be endothermic and non-spontaneous in nature.

For mechanism of adsorption by hydroxyl groups Eqs. (26) and (27):

$$CDS - OH + OH^- \rightarrow CDS - O^- + H_2O \quad (26)$$

$$CDS - O^- + CV^+Cl^- \rightarrow CDS - O - CV + Cl^- \quad (27)$$

Carboxyl group contribution towards adsorption is represented given in Eq. (28):

$$CDS - COO^- + CV^+Cl^- \rightarrow CDS - COO - CV + Cl^- \quad (28)$$

In above mechanism, CDS represents *Cedrus deodara* sawdust and CV^+ Cl^- represents cationic crystal violet dye with molecular formulae = $C_{25}H_{30}ClN_3$. This mechanism is further confirmed by decrease in removal percentage at low solution pH where release of Cl^- is suppressed resulting in decrease in removal percentage of dye. Besides electrostatic forces of attraction, formation of hydrogen bonds between OH^- groups of *Cedrus deodara* sawdust (CDS) and amine group of crystal violet dye also aid in adsorption of dye molecules. This mechanism has also been reported earlier in crystal violet dye removal using *Tectonagrandis* sawdust. Probability of intraparticle pore diffusion of crystal violet dye can be determined from intraparticle diffusion kinetic model. Since line of this plot does not pass from origin hence it confirmed the involvement of both film and intraparticle diffusion in dye removal.

From above discussion, it became clear that removal of crystal violet dye involves following steps:

- Movement of crystal violet dye molecules from solution to the surface of CDS.
- Diffusion of dye molecules through the boundary layer to the surface of adsorbent.
- Adsorption of dye molecules on adsorbent surface by:
- Strong electrostatic interactions between negatively charged adsorbent surface (OH^- and COO^-) and positively charged dye molecules (CV^+Cl^-)
- H-bonding between OH^- groups of adsorbent and amine groups of dye molecules [27].

Complete mechanism of crystal violet dye (an adsorbate) adsorption on the surface of *Cedrus deodara* sawdust

Table 4
Calculated thermodynamic parameters

ΔG (kJ mol^{-1})	ΔH (kJ mol^{-1})	ΔS (J mol^{-1} K^{-1})
–0.7726		
–0.7926		
–0.8162		
–0.8306	7.5708	0.06645
–0.8456		
–0.8574		

(as an adsorbent) is given in Fig. 19 showing the involvement of both electrostatic (due to hydroxyl and carboxyl groups of adsorbents with chlorine ions of crystal violet dye) and hydrogen bonding (between amine groups of crystal violet dye and hydroxyl groups of *Cedrus deodara* sawdust) in dye adsorption [27].

6. Regeneration study

Adsorbent (*Cedrus deodara* sawdust) and adsorbate (crystal violet dye in this case) recovery are significant characteristics of water treatment since it shows that the process is economically feasible [28]. Desorption study of crystal violet dye was carried out using HNO_3 as desorbing agent. For recovery of adsorbent and dye, fixed amount of dye loaded adsorbent was shaken with 1 molar nitric acid solution with 20 min of contact time. As a result, 93% of crystal violet dye and adsorbent were recovered and became available for further production and treatment, respectively (results of regeneration study are shown in Table S14). However, removal efficacy of adsorbent decrease after regeneration as it is obvious from experiment carried out using regenerated adsorbent. The same adsorption experiments were conducted at optimized parameters such as solution pH of 12, 0.4 g of adsorbate concentration with 20 ppm dye concentration for 30 min. Results indicate 70% of crystal violet dye removal showing that *Cedrus deodara* sawdust is a promising adsorbent for crystal violet dye removal.

6.1. Mechanism of desorption

Mineral acids are highly efficient desorbing agents especially for cationic dyes such as crystal violet dye. When 1 M HNO_3 solution was added into the solution of loaded dye, it causes decrease in solution pH. Low pH cause surface of the adsorbent to be positively charged hence bond between crystal violet dye and surface of adsorbent break due to repulsion of like charges (i.e., positive charge of cationic crystal violet dye and positive charge on surface of adsorbent). Thus, both dye and adsorbent were recovered for future use.

7. Conclusions

This analysis reflects aptitude of *Cedrus deodara* sawdust as low priced and environmentally sound adsorbent for exclusion of toxic crystal violet colorant from wastewater via adsorption technique. Main objectives of this study are to investigate the potential of *Cedrus deodara* sawdust for removal of toxic crystal violet dye and to stimulate the best experimental conditions. Adsorbent was characterized by FTIR and SEM techniques.

FTIR analysis showed that the functional groups such as carboxyl, hydroxyl and carbonyl etc. contribute mainly to crystal violet dye adsorption onto the surface of *Cedrus deodara* sawdust since peaks of these functional groups involved in dye uptake became diminished after dye uptake. Both electrostatic (due to hydroxyl and carboxyl groups of adsorbents with chlorine ions of crystal violet dye) and hydrogen bonding (between amine groups of crystal violet and hydroxyl groups of *Cedrus deodara* sawdust) are involved in dye adsorption. SEM analysis showed that the surface of adsorbent is highly rough, diverse, and porous indicating increased superficial zone of adsorbent accessible for adsorption of crystal violet dye. After adsorption, these pores were occupied by dye molecules resulting in dye exclusion.

Adsorption parameters, isotherms, kinetic equations, and thermodynamic parameters have been studied. Experiments were performed (in batch mode) to investigate the effects of various parameters on dye removal. These parameters include size of adsorbent, pH, adsorbent dose, contact time, adsorbate dosage and temperature. Maximum

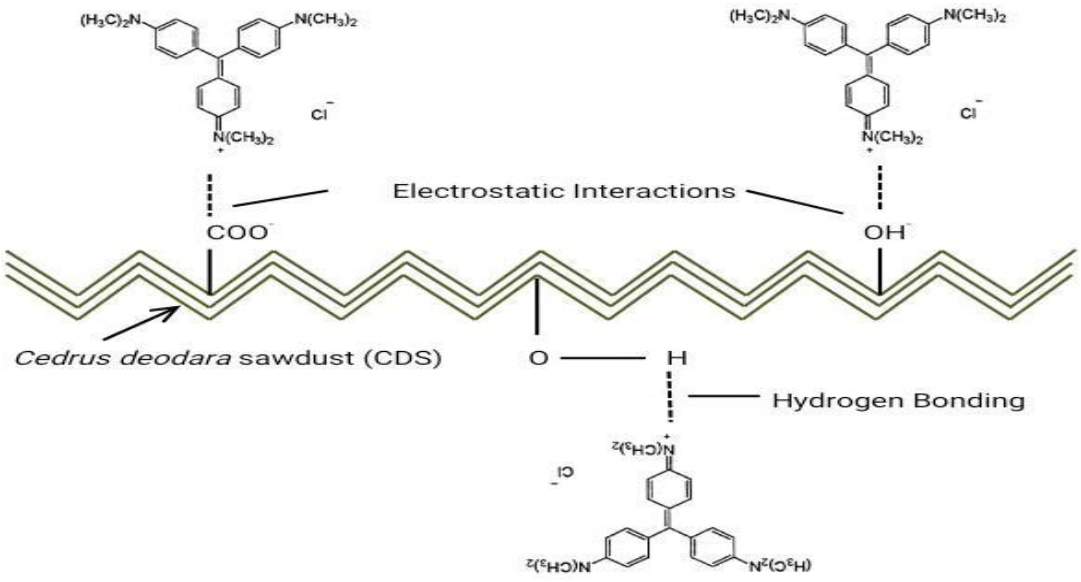

Fig. 19. Mechanism of adsorption of crystal violet dye molecules on *Cedrus deodara* sawdust.

amount of dye (i.e., 99.21%) has been removed at optimized conditions, that is, 210 mesh size, 50°C temperature, pH 12, 0.4 g adsorbent, 20 ppm adsorbate concentration with contact time of 30 min.

Concentration data from experiment has been analyzed using various isotherm models to determine the best suited isotherm model in the adsorption process. Isotherm models applied here include, Langmuir, Freundlich and Dubinin–Radushkevich isotherm. Data fits best to Langmuir isotherm and value of R^2 for Langmuir model was 0.9994 which is very close to unity demonstrating that current process of adsorption is promising. Various kinetic models, that is, pseudo-first-order, pseudo-second-order and intraparticle diffusion models have been applied and discussed. Process obeys pseudo-second-order kinetics. The value of regression coefficient (R^2) for pseudo-second-order was 0.9999 which shows very good rate of adsorption. This confirms that adsorption procedure of crystal violet on surface of *Cedrus deodara* is chemical adsorption. Thermodynamic factors show that the current process was of endothermic type associated with increase in entropy. Positive ΔS and negative ΔG confirm strong solute-solvent interactions.

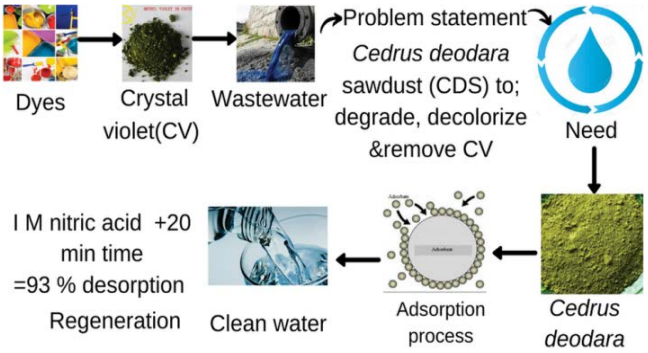

Fig. 20. Graphical abstract of the adsorption process, that is, adsorption of crystal violet dye onto the surface of *Cedrus deodara* sawdust (easily available and low-cost adsorbent). Removal of such kind of pollutants is crucial for the availability of safe and clean drinking water. Desorption study resulted in regeneration of both adsorbent and adsorbate for future use.

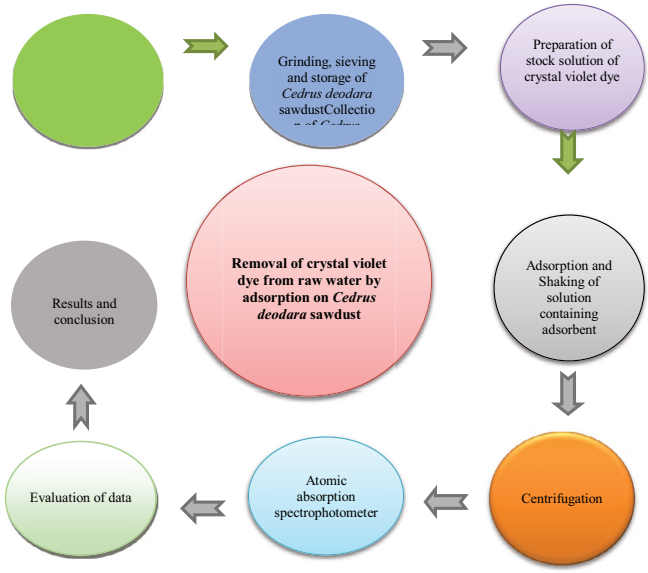

Fig. 21. Complete steps for crystal violet dye removal from wastewater onto the surface of *Cedrus deodara* sawdust by adsorption method.

Applicability of developed procedure with tap water containing various anions and cations like Cl^-, PO_4^{2-}, CO_3^{2-}, Na^+ and K^+ ions etc. was carried out using optimized conditions, that is, pH value of 12, 0.4 g of adsorbent dose, providing adsorption time of 30 min with 20 ppm of adsorbate concentration. About 92.32% of crystal violet dye has been removed onto the surface of *Cedrus deodara* sawdust using tap water indicating that *Cedrus deodara* sawdust is an auspicious adsorbent for crystal violet dye removal from water.

On the basis of above discussion, it became clear that low cost and easily available *Cedrus deodara* sawdust has great potential for degradation, decolorization and removal of hazardous crystal violet dye from raw water thus leading to water purification and protecting natural sources such as water, air and land. Graphical abstract of the adsorption process, that is, adsorption of crystal violet dye onto the surface of *Cedrus deodara* sawdust is shown in Fig. 20 and complete steps for crystal violet dye removal from wastewater onto the surface of *Cedrus deodara* sawdust by adsorption method is given in Fig. 21.

8. Recommendation

To test the proficiency of *Cedrus deodara* sawdust towards exclusion of crystal violet dye from wastewater, the model dye could be replaced by actual industrial waste.

Acknowledgments

Foremost, all praise to Almighty Allah for blessing me with strength and enabling me to successfully complete this work.

I would like to acknowledge my nearest and dearest parents and family for their endless love, support, and encouragement. I would like to manifest my special appreciations to my supervisor, my mentor, Dr. Tariq Javed, Lecturer, Department of Chemistry, University of Sahiwal, Sahiwal, Punjab, Pakistan, for his valuable guidance and support in completing my research work. I would also like to widen my appreciation to Dr. M. Nasir Afzal, Vice Chancellor, University of Sahiwal, Sahiwal, Punjab, Pakistan, for providing me with all the facility that was required. I would like to acknowledge the facilities and technical support received from Department of Chemistry, University of Sahiwal, Sahiwal, Punjab, Pakistan.

Symbols

q_t — Adsorption capacity at time 't', mg g^{-1}
q_e — Adsorption capacity at equilibrium, mg g^{-1}
C_0 — Initial concentration of dye, mg L^{-1}
C_e — Equilibrium concentration of dye, mg L^{-1}
V — Volume of dye solution taken, ml
M — Mass of adsorbent, g
pH_{pzc} — Point of zero charge
k_f — Pseudo-first-order rate constant, min^{-1}

K_s — Pseudo-second-order rate constant, g mg^{-1} min^{-1}
K_L — Langmuir constant, dm^{-3} mol^{-1}
b — Langmuir adsorption equilibrium constant, L mol^{-1}
R_L — Dimensionless constant separation factor parameter
K_F — Freundlich rate constant/adsorption capacity, mg g^{-1}
n — Intensity of adsorption, L g^{-1}
β — Constant related to adsorption energy or activity coefficient, KJ^2 mol^{-2}
q_{DR} — Imaginary inundation capacity
ε^2 — Polyanyi potential, KJ mol^{-1}
K_{id} — Intra-particle rate constant, mg g^{-1} $min^{-1/2}$
$C_{ad,s}$ — Quantity of adsorbate adsorbed on solid at equipoise, mg L^{-1}
$C_{Eq,L}$ — Quantity of adsorbate left over in solution at equipoise, mg L^{-1}
T — Temperature, K
R — Universal gas constant = 8.31 J mol^{-1} K^{-1}
ΔG — Change in Gibbs free energy, KJ mol^{-1}
ΔH — Change in enthalpy, KJ mol^{-1}
ΔS — Change in entropy, J mol^{-1} K^{-1}

References

[1] P.V. Nidheesh, R. Gandhimathi, S.T. Ramesh, T.S.A. Singh, Adsorption and desorption characteristics of crystal violet in bottom ash column, J. Urban Environ. Eng., 6 (2012) 18–29.
[2] K. Singh, P. Kumar, R. Srivastava, An overview of textile dyes and their removal techniques: Indian perspective, Pollut. Res., 36 (2017) 790–797.
[3] S. Sharma, A. Kaur, Various methods for removal of dyes from industrial effluents - a review, Indian J. Sci. Technol., 11 (2018) 1–21.
[4] C. Mahamadi, E. Mawere, Continuous flow biosorptive removal of methylene blue and crystal violet dyes using alginate–water hyacinth beads, Cogent Environ. Sci., 5 (2019) 1594513, doi: 10.1080/23311843.2019.1594513.
[5] F.M.D. Chequer, G.A.R. de Oliveira, E.R.A. Ferraz, J.C. Cardoso, M.V.B. Zanoni, D.P. de Oliveira, Chapter 6 – Textile Dyes: Dyeing Process and Environmental Impact, In: Eco-friendly Textile Dyeing and Finishing, INTECH, United States, 2013, pp. 151–176.
[6] S. El Harfi, A. El Harfi, Classifications, properties and applications of textile dyes: a review, Appl. J. Environ. Eng. Sci., 3 (2017) 00000–00003 N° 00003 (02017) 00311–00320, doi: 10.48422/IMIST.PRSM/ajees-v3i3.9681.
[7] S. Arora, Textile dyes: it's impact on environment and its treatment, J. Biorem. Biodegrad., 5 (2014) e146, doi: 10.4172/2155-6199.1000e146.
[8] R. Srivastava, I.R. Sofi, Impact of Synthetic Dyes on Human Health and Environment, In: Impact of Textile Dyes on Public Health and the Environment, IGI Publisher, USA, 2020, pp. 146–161.
[9] N.J. Okorocha, C.K. Enenebeaku, M.O. Chijioke-Okere, C.E. Ohaegbulam, C.E. Ogukwe, Adsorptive removal of crystal violet using agricultural waste: equilibrium, kinetic and thermodynamic studies, Am. J. Eng. Res., 8 (2019) 38–51.
[10] Y. Miyah, A. Lahrichi, M. Idrissi, S. Boujraf, H. Taouda, F. Zerrouq, Assessment of adsorption kinetics for removal potential of crystal violet dye from aqueous solutions using moroccan pyrophyllite, J. Assoc. Arab Univ. Basic Appl. Sci., 23 (2017) 20–28.
[11] M. Abbaz, The removal and desorption of two toxic dyes from aqueous solution by hydroxylated hematite sand: kinetics and equilibrium, J. Appl. Chem. Environ. Prot., 2 (2017) 31–52.
[12] S. Madhavakrishnan, K. Manickavasagam, R. Vasanthakumar, K. Rasappan, R. Mohanraj, S. Pattabhi, Adsorption of crystal violet dye from aqueous solution using *Ricinus communis* pericarp carbon as an adsorbent, E-J. Chem., 6 (2009) 1109–1116.
[13] A. Nasar, S. Shakoor, Remediation of Dyes from Industrial Wastewater using Low-cost Adsorbents, In: Applications of Adsorption and Ion Exchange Chromatography in Waste Water Treatment, Materials Research Forum LLC, 2 Millersville, PA, 018.
[14] L.K. Akinola, A.M. Umar, Adsorption of crystal violet onto adsorbents derived from agricultural wastes: kinetic and equilibrium studies, J. Appl. Sci. Environ. Manage., 19 (2015) 279–288.
[15] A. Mittal, J. Mittal, A. Malviya, D. Kaur, V.K. Gupta, Adsorption of hazardous dye crystal violet from wastewater by waste materials, J. Colloid Interface Sci., 343 (2010) 463–473.
[16] H.M. Ali, S.F. Shehata, K.M.A. Ramadan, Microbial decolorization and degradation of crystal violet dye by *Aspergillus niger*, Int. J. Environ. Sci. Technol., 13 (2016) 2917–2926.
[17] P. Raval, V. Priti, Potential of Anionic Surfactant Modified Alumina in Removal of Crystal Violet from Aqueous Solution, Shodhganga INFLIBNET Center, India, pp. 187–245.
[18] S.M. Yakout, M.S. Ali, Removal of the hazardous crystal violet dye by adsorption on corncob-based and phosphoric acid-activated carbon, Part. Sci. Technol., 33 (2015) 621–625.
[19] Z.U. Zango, S.S. Imam, Evaluation of microcrystalline cellulose from groundnut shell for the removal of crystal violet and methylene blue, Nanosci. Nanotechnol., 8 (2018) 1–6.
[20] W. Yao, W.Q. Zhu, Y. Wu, X.Y. Wang, T. Jianati, Removal of crystal violet dye from wastewater by solidified landfilled sludge and its modified products, Pol. J. Environ. Stud., 24 (2015) 777–785.
[21] A. Wathukarage, I. Herath, M.C.M. Iqbal, M. Vithanage, Mechanistic understanding of crystal violet dye sorption by woody biochar: implications for wastewater treatment, Environ. Geochem. Health,. 41 (2019) 1647–1661.
[22] V. Katheresan, J. Kansedo, S.Y. Lau, Efficiency of various recent wastewater dye removal methods: a review, J. Environ. Chem. Eng., 6 (2018) 4676–4697.
[23] K.D. Mojsov, D. Andronikov, A. Janevski, A. Kuzelov, S. Gaber, The application of enzymes for the removal of dyes from textile effluents, Adv. Technol., 5 (2016) 81–86.
[24] W. Handayani, A.I. Kristijanto, A.I.R. Hunga, Are natural dyes eco-friendly? a case study on water usage and wastewater characteristics of batik production by natural dyes application, Sustainable Water Resour. Manage., 4 (2018) 1011–1021.
[25] M.T. Amin, A.A. Alazba, U. Manzoor, A review of removal of pollutants from water/wastewater using different types of nanomaterials, Adv. Mater. Sci. Eng., 2014 (2014) 825910, doi: 10.1155/2014/825910.
[26] A. Mosbah, H. Chouchane, S. Abdelwahed, A. Redissi, M. Hamdi, S. Kouidhi, M. Neifar, A. Slaheddine Masmoudi, A. Cherif, W. Mnif, Peptides fixing industrial textile dyes: a new biochemical method in wastewater treatment, J. Chem., 2019 (2019) 5081807, doi: 10.1155/2019/5081807.
[27] F. Mashkoor, A. Nasar, Inamuddin, A.M. Asiri, Exploring the reusability of synthetically contaminated wastewater containing crystal violet dye using *Tectona grandis* sawdust as a very low-cost adsorbent, Sci. Rep., 8 (2018) 8314, doi: 10.1038/s41598-018-26655-3.
[28] J. Tariq, K. Nasir, M.L. Mirza, Kinetics, equilibrium and thermodynamics of cerium removal by adsorption on low-rank coal, Desal. Water Treat., 89 (2017) 240–249.
[29] K. Hayat, Studies on Sorption of Methylene Blue Over *Cedrus deodara* Saw, Master of Philosophy in Chemistry, The Islamia University of Bahawalpur, 2017, p. 97.
[30] M.T. Yagub, T.K. Sen, S. Afroze, H.M. Ang, Dye and its removal from aqueous solution by adsorption: a review, Adv. Colloid Interface Sci., 209 (2014) 172–184.
[31] M.K. Dahri, M.R.R. Kooh, L.B.L. Lim, *Artocarpus odoratissimus* (tarap) core as an adsorbent for the removal of crystal violet dye from aqueous solution, J. Mater. Environ. Sci., 8 (2017) 3706–3717.
[32] L.B.L. Lim, A. Usman, M.H. Hassan, N.A.H. Mohamad Zaidi, Tropical wild fern (*Diplazium esculentum*) as a new and effective

low-cost adsorbent for removal of toxic crystal violet dye, J. Taibah Univ. Sci., 14 (2020) 621–627.
[33] M.A. Gabal, E.A. Al-Harthy, Y.M. Al Angari, M.A. Salam, MWCNTs decorated with $Mn_{0.8}Zn_{0.2}Fe_2O_4$ nanoparticles for removal of crystal-violet dye from aqueous solutions, Chem. Eng. J., 255 (2014) 156–164.
[34] H.I. Chieng, L.B.L. Lim, N. Priyantha, Enhancement of crystal violet dye adsorption on *Artocarpus camansi* peel through sodium hydroxide treatment, Desal. Water Treat., 58 (2017) 320–331.
[35] L.B.L. Lim, P. Namal, K.J. Mek, N.A.H.M. Zaidi, Potential use of *Momordica charantia* (bitter gourd) waste as a low-cost adsorbent to remove toxic crystal violet dye, Desal. Water Treat., 82 (2017) 121–130.
[36] M. Alshabanat, G. Alsenani, R. Almufarij, Removal of crystal violet dye from aqueous solutions onto date palm fiber by adsorption technique, J. Chem., 2013 (2013) 210239, doi: 10.1155/2013/210239.
[37] Q.-Z. Zhai, Studies of adsorption of crystal violet from aqueous solution by nano mesocellular foam silica: Process equilibrium, kinetic, isotherm, and thermodynamic studies, Water Sci. Technol., 81 (2020) 2092–2108.

Supporting information

Table S1
Results of experiment to study the effects of solution pH (experimental conditions: pH = variable (1–12); C_0 = 10 ppm; adsorbent dose = 0.25 g; contact time = 20 min; temperature = 25°C)

pH	A_i	A_f	C_e	% age removal
1	0.36	0.31	0.034	11.94
2	0.57	0.18	0.020	67.41
3	0.65	0.15	0.017	75.98
4	0.89	0.19	0.020	78.37
5	0.91	0.19	0.020	79.23
6	0.82	0.15	0.016	81.18
7	0.81	0.15	0.016	81.25
8	1.02	0.18	0.020	81.76
9	0.72	0.11	0.011	84.58
10	0.79	0.12	0.013	84.67
11	0.47	0.06	0.006	87.23
12	0.36	0.04	0.004	88.88

Table S2
Results of experiment to study the effects of adsorbent dosage (experimental conditions: adsorbent dose = variable (0.1–1.0 g); pH = 12; C_0 = 40 ppm; contact time = 20 min; temperature = 25°C)

Adsorbent dose (g)	A_i	A_f	C_e	% age exclusion
0.1	1.88	0.21	5.27	88.38
0.2	1.88	0.06	1.56	96.55
0.4	1.88	0.03	0.89	98.03
0.5	1.88	0.03	0.81	98.19
0.6	1.88	0.03	0.81	98.19
0.8	1.88	0.04	1.08	97.61
1	1.88	0.04	1.08	97.61

Table S3
Results of experiment to study the effects of contact time (experimental conditions: contact time = variable (05–120 min); pH = 12; adsorbent dose = 0.4 g; C_0 = 80 ppm; temperature = 25°C)

Contact time (min)	A_i	A_f	C_e	% age exclusion
5	1.845	0.134	7.401	92.699
10	1.845	0.131	7.203	92.894
20	1.845	0.124	6.818	93.273
30	1.845	0.117	6.428	93.658
40	1.845	0.11	6.043	94.037
50	1.845	0.101	5.602	94.473
60	1.845	0.096	5.302	94.769
80	1.845	0.087	4.802	95.262
100	1.845	0.078	4.302	95.756
120	1.845	0.069	3.802	96.249

Table S4
Results of experiment to study the effects of dye concentration (experimental conditions: C_0 = variable (05–100 ppm); pH = 12; adsorbent dose = 0.4 g; contact time = 30 min; temperature = 25°C)

Adsorbate conc. (ppm)	A_i	A_f	C_e	% age removal
5	1.80	0.0047	0.360	99.737
10	1.82	0.008	0.634	99.543
20	1.86	0.013	1.007	99.290
30	1.88	0.016	1.250	99.128
40	1.90	0.018	1.430	99.014
50	1.90	0.020	1.570	98.920
60	1.90	0.022	1.679	98.847
80	1.91	0.023	1.820	98.753
100	1.91	0.025	1.930	98.678

Table S5
Results of experiment to study the effects of temperature (experimental conditions: temperature = variable (0°C–50°C); pH = 12; adsorbent dose = 0.4 g; contact time = 30 min; C_0 = 200 ppm)

Temperature °C	A_i	A_f	C_e	% age removal
0	1.915	0.024	1.900	98.699
10	1.915	0.022	1.687	98.845
20	1.915	0.019	1.465	98.997
30	1.915	0.017	1.343	99.080
40	1.915	0.016	1.229	99.159
50	1.915	0.015	1.145	99.216

Table S6
Investigational statistics for pseudo-first-order kinetics

Time (t) min	C_e (mg L^{-1})	q_t (mg g^{-1})	$\log(q_e - q_t)$
5	7.401	1.814	–1.045
10	7.203	1.819	–1.070
20	6.818	1.829	–1.122
30	6.428	1.839	–1.182
40	6.043	1.848	–1.251
50	5.602	1.859	–1.346
60	5.302	1.867	–1.425
80	4.802	1.879	–1.602
100	4.302	1.892	–1.903
120	3.802	q_e = 1.904	–10.26

Table S7
Investigational statistics for pseudo-second-order kinetics

Time (t) min	C_e (mg L^{-1})	q_t (mg g^{-1})	t/q_t
5	7.401	1.814	2.754
10	7.203	1.819	5.494
20	6.818	1.829	10.93
30	6.428	1.839	16.31
40	6.043	1.848	21.63
50	5.602	1.859	26.88
60	5.302	1.867	32.12
80	4.802	1.879	42.55
100	4.302	1.892	52.84
120	3.802	1.904	62.99

Table S8
Investigational statistics for intraparticle diffusion model

Time (t) min	$t^{1/2}$	C_e (mg L^{-1})	q_t (mg g^{-1})
5	2.23	7.401	1.814
10	3.16	7.203	1.819
20	4.47	6.818	1.829
30	5.47	6.428	1.839
40	6.32	6.043	1.848
50	7.07	5.602	1.859
60	7.74	5.302	1.867
80	8.94	4.802	1.879
100	10.0	4.302	1.892
120	10.9	3.802	1.904

Table S9
Calculation of R_L values

b	Initial dye conc.	R_L
1.66×10^{-5}	1.22555E-05	1
1.66×10^{-5}	2.45111E-05	1
1.66×10^{-5}	4.90221E-05	1.000000001
1.66×10^{-5}	7.35332E-05	1.000000001
1.66×10^{-5}	9.80443E-05	1.000000002
1.66×10^{-5}	0.000122555	1.000000002
1.66×10^{-5}	0.000147066	1.000000002
1.66×10^{-5}	0.000196089	1.000000003
1.66×10^{-5}	0.000245111	1.000000004

Table S10
Experimental data for Langmuir isotherm model

Initial conc. (ppm) or mg L^{-1}	Initial conc. (mol L^{-1})	C_e (ppm)	C_e (mol L^{-1})	$C_{ads} = (C_0 - C_e)V/m$ (mol g^{-1})	C_e/C_{ads} (g L^{-1})
5	1.22×10^{-5}	0.360	8.83×10^{-7}	2.84×10^{-7}	3.106
10	2.45×10^{-5}	0.634	1.55×10^{-6}	5.73×10^{-7}	2.709
20	4.90×10^{-5}	1.007	2.46×10^{-6}	1.16×10^{-6}	2.122
30	7.35×10^{-5}	1.250	3.06×10^{-6}	1.76×10^{-6}	1.739
40	9.80×10^{-5}	1.430	3.50×10^{-6}	2.36×10^{-6}	1.483
50	0.00012	1.570	3.84×10^{-6}	2.96×10^{-6}	1.296
60	0.00014	1.679	4.11×10^{-6}	3.57×10^{-6}	1.151
80	0.00019	1.820	4.46×10^{-6}	4.79×10^{-6}	0.931
100	0.00024	1.930	4.73×10^{-6}	6.00×10^{-6}	0.787

Table S11
Experimental data for Freundlich isotherm model

Initial conc. (ppm)	Initial conc. (mol L^{-1})	C_e (mol L^{-1})	$C_{ads} = (C_0 - C_e)V/m$ (mol g^{-1})	$\log C_e$	$\log C_{ads}$
5	1.22×10^{-5}	8.83×10^{-7}	2.84×10^{-7}	–6.05	–6.54
10	2.45×10^{-5}	1.55×10^{-6}	5.73×10^{-7}	–5.80	–6.24
20	4.90×10^{-5}	2.46×10^{-6}	1.16×10^{-6}	–5.60	–5.93
30	7.35×10^{-5}	3.06×10^{-6}	1.76×10^{-6}	–5.51	–5.75
40	9.80×10^{-5}	3.50×10^{-6}	2.36×10^{-6}	–5.45	–5.62
50	0.00012	3.84×10^{-6}	2.96×10^{-6}	–5.41	–5.52
60	0.00014	4.11×10^{-6}	3.57×10^{-6}	–5.38	–5.44
80	0.00019	4.46×10^{-6}	4.79×10^{-6}	–5.35	–5.31
100	0.00024	4.73×10^{-6}	6.00947E-06	–5.324	–5.221

Table S12
Experimental data for Dubinin–Radushkevich model

Initial conc. (ppm)	C_e (mol L^{-1})	$C_{ads} = (C_0 - C_e)V/m$ (mol g^{-1})	$\ln C_{ads}$	$\varepsilon = RT\ln\{1+(1/C_e)\}$	ε^2
5	8.83×10^{-7}	2.84×10^{-7}	–15.07	2.31	5.37
10	1.55×10^{-6}	5.73×10^{-7}	–14.37	2.22	4.94
20	2.46×10^{-6}	1.16×10^{-6}	–13.66	2.14	4.60
30	3.06×10^{-6}	1.76×10^{-6}	–13.24	2.11	4.45
40	3.50×10^{-6}	2.36×10^{-6}	–12.95	2.08	4.36
50	3.84×10^{-6}	2.96×10^{-6}	–12.72	2.07	4.29
60	4.11×10^{-6}	3.57×10^{-6}	–12.54	2.06	4.25
80	4.46×10^{-6}	4.79×10^{-6}	–12.24	2.04	4.19
100	4.73×10^{-6}	6.00×10^{-6}	–12.02	2.03	4.15

Table S13
Investigational statistics for thermodynamic parameters

C_e (mol L^{-1})	$C_a = (C_i - C_e)$ (mol L^{-1})	T (°C)	T (K)	$1/T$	$K_c = C_a/C_e$	$\ln K_c$
4.65×10^{-6}	0.0004855	0	273	0.0036	104.22	4.64
4.13×10^{-6}	0.0004860	10	283	0.0035	117.55	4.76
3.59×10^{-6}	0.0004866	20	293	0.0034	135.45	4.90
3.29×10^{-6}	0.0004869	30	303	0.0033	147.86	4.99
3.01×10^{-6}	0.0004872	40	313	0.0031	161.73	5.08
2.80×10^{-6}	0.0004874	50	323	0.0030	173.66	5.15

Table S14
Results of regeneration study

Adsorbent	*Cedrus deodara* sawdust
Adsorbate (dye)	Crystal violet
Chemical used for desorption	1 M HNO_3
Contact time (min)	20 min
% age removal	93%